NANOSYSTEMS:
PHYSICS, CHEMISTRY, MATHEMATICS

Original article

Kaldante Y.D., Chaskar M.G. *Nanosystems: Phys. Chem. Math.*, 2023, **14** (1), 98–106.
http://nanojournal.ifmo.ru
DOI 10.17586/2220-8054-2023-14-1-98-106

A comparative study of photocatalytic degradation of Xylenol Orange dye under natural sunlight over ZnO nanoparticles synthesized via mechanochemical and hydrothermal assistance routes

Yogeshwar D. Kaldante[1,a], Manohar G. Chaskar[2,b]

[1]Department of Chemistry, PDEA's Annasaheb Waghire College, Otur, Pune, Maharashtra – 412409, India
[2]Department of Chemistry, PDEA's Prof. Ramkrishna More College, Akurdi, Maharashtra – 411044, India

[a]ydkaldante@gmail.com, [b]chaskarmanohar@gmail.com

Corresponding author: Yogeshwar D. Kaldante, ydkaldante@gmail.com

ABSTRACT Current work confers mechanochemical and hydrothermal syntheses of ZnO, its characterization and photocatalytic applications. Mechanochemical and hydrothermal assisted syntheses of ZnO involve two stages viz. formation of precursors followed by its calcination. The suitable calcination temperature for precursor materials to get ZnO was obtained by TG-DTA and FT-IR Spectroscopic study; XRD data of these samples specified hexagonal wurtzite crystallite structures of ZnO. FESEM photographs of mechanochemically and hydrothermally synthesize ZnO confirmed nanocrystalline hexagonal granular and stacked block-like particle morphologies respectively. EDX spectra of these samples support their elemental purity. The UV-DRS study was used to measure the optical band gap of ZnO samples. Optical properties of ZnO samples were also studied with room temperature PL spectra. Photocatalytic applications of aforementioned ZnO samples were investigated with Xylenol Orange as a model organic dye. The PCD efficiency of ZnO was estimated in terms of percent degradation reference to various operating factors.

KEYWORDS zinc oxide, Xylenol Orange, mechanochemical, hydrothermal, PCD efficiency

ACKNOWLEDGEMENTS Authors are exclusively grateful to PDEA's Annasaheb Waghire College, Otur for providing their continuous and valuable support, in terms of amenities like laboratories for all experimental work and library for the literature review. Authors are also thankful to PDEA's Baburaoji Gholap College, Sangvi and CIF, SPPU, Pune for giving instrumental facilities for the characterization of materials.

FOR CITATION Kaldante Y.D., Chaskar M.G. A comparative study of photocatalytic degradation of Xylenol Orange dye under natural sunlight over ZnO nanoparticles synthesized via mechanochemical and hydrothermal assistance routes. *Nanosystems: Phys. Chem. Math.*, 2023, **14** (1), 98–106.

1. Introduction

Wide range of applications of nano-sized semiconducting materials is available due to their mechanical, electrical, chemical and optical properties which can be tuned by altering their particle dimensions [1]. Metal oxides are established as promising candidates for their applications in the fields such as catalysis [2], sensing [3], energy storage and conversion [4, 5], optoelectronic devices [6], memory arrays [7], biomedical application [8] and acoustic wave devices [9]. ZnO is a key material of researcher interest because of its exceptional physico-chemical properties among semiconductor metal oxide. ZnO possess direct wide band gap (3.37 eV) with high exciton binding energy (60 meV) [1, 10]. ZnO shows strong piezoelectric, pyroelectric and optoelectronic properties [10, 11]. Eco-friendly and biocompatible nature and good thermal stability make ZnO most hopeful contestant for electronic and optoelectronic applications [11]. Nanosized ZnO materials can be gained by using various synthetic routes for instance mechanochemical [12], chemical precipitation [13], solution combustion [14], sol-gel method [15], hydrothermal synthesis [1, 10, 16], etc. Within these methods of ZnO synthesis mechanochemical and hydrothermal methods are quite suitable to control the particle size. Some advantages associated with mechanochemical method are its simplicity, low cost, eco-friendly nature and suitability for large-scale production of ZnO [17]. In addition to this, it is suitable for controlling the growth and nucleation of nanoparticles [17]. Hydrothermal method is also linked with quite a lot of advantages like low cost, large area uniform NPs production, eco-friendliness, catalyst-free growth of NPs, use of simple equipment, less hazardous [1], etc. The morphology and size of NPs can be controlled by adjusting concentration of precursors, reaction time, calcination temperature, etc. Hence, both these process are recognized to obtain the nanomaterials with diverse morphologies and particle sizes. Advanced Oxidation Processes (AOPs) are the efficient tool for the environmental technology. Within AOPs heterogeneous photocatalysis is one of the well-recognized and best substitutes for the conventional methods of water treatment [18]. Heterogeneous photocatalysis is the most efficient and economical method for the complete mineralization of organic contaminants to less and / or

non-toxic end products [19]. Midst various metal oxide photocatalysts, ZnO is extensively investigated material for its photocatalytic applications due to low cost, nontoxic nature and high photochemical reactivity [20].

In the current work, we have conferred mechanochemical and hydrothermal assisted synthesis of ZnO NPs and their thorough characterization by several techniques. The photocatalytic activities of these ZnO NPs photocatalysts were verified by means of degradation of xylenol orange dye (Fig. 1). The rate of photocatalytic degradation of xylenol orange was studied with reference to the operating factors like pH of dye solution, photocatalyst quantity, dye concentration, irradiation time, etc. The aim of the present research work is to study the effective methods of precursor preparation in the earlier stage prior to calcination during synthesis of ZnO NPs and its effect on the photocatalytic degradation of Xylenol Orange (Sulphonephthalein) dye as a model dye. Since sulphonephthalein dyes constitutes one of the large class of dyes used in various applications.

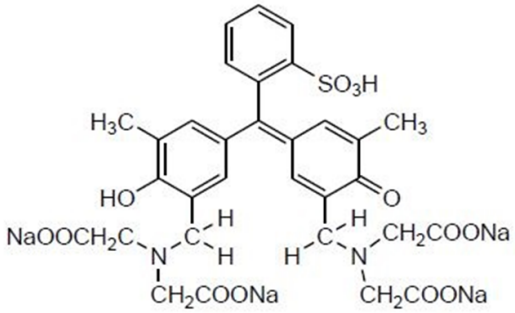

FIG. 1. Chemical structure of the Xylenol Orange dye molecule

2. Experimental

2.1. Materials

$Zn(CH_3COO)_2 \cdot 2H_2O$ (assay 99.5 %), $H_2C_2O_4 \cdot 2H_2O$ (assay 99.0 %), Xylenol Orange (assay 99.0 %), liquor NH_3 (25 % w/w), TiO_2 (Degussa P25) (assay 99.5 %) and additional necessary chemicals used as-received during current work were AR grade reagents acquired from S.D. Fine Chemicals Limited, India. Distilled water used to prepare all the allied experimental solutions. Wherever needed, pH of the related solutions was agreed to desired values with NaOH (0.05 M) and HCl (0.05 M).

2.2. Synthesis of photocatalyst

2.2.1. Mechanochemical synthesis of ZnO. Zinc oxide (ZnO) was gained by two step method. Initially $ZnC_2O_4 \cdot 2H_2O$ precursor was obtained by mechanical hand grinding of a mixture of 10.975 gm of $Zn(CH_3COO)_2 \cdot 2H_2O$ with 6.93 gm of $H_2C_2O_4 \cdot 2H_2O$ in agate mortar for about 30 minutes at room temperature. Secondly $ZnC_2O_4 \cdot 2H_2O$ precursor was calcined at 450 °C for 4 hours in air atmosphere to give formation of ZnO powder [21–23].

2.2.2. Hydrothermal assisted synthesis of ZnO. Zinc Oxide (ZnO) was produced as mentioned. 10 ml liquor NH_3 was added very slowly in a dropwise mode under vigorous magnetic stirring for the period of about 1 hour to the 100 ml solution of 0.5 M $Zn(CH_3COO)_2 \cdot 2H_2O$. The pH of the reaction mixture was assured to be nearly 9 to 9.5. To ensure homogeneous phase, the resultant white suspension was furthermore stirred for another 1 hour, it was then transferred to the teflon-lined container in a hydrothermal reactor. Reactor was correctly sealed and kept at 100 °C for 4 hours under autogenous pressure. It was then naturally allow attaining room temperature. Then the resultant white residue of hydrated zinc oxide was filtered and washed with water followed by ethanol and finally dried at 100 °C and the same is calcined at 450 °C for 4 hours in air atmosphere to ensure formation of ZnO.

2.3. Equipments

The correct calcination temperature for the formation of ZnO from precursors in case of mechanochemical and hydrothermal assisted synthesis was gained by thermogravimetric analysis machine (Shimadzu, TG-DTG-60H) and FT-IR (PerkinElmer UATR Spectra Two) spectrometer. The XRD patterns of above mentioned ZnO samples was produced with X-ray Diffractometer (Rikagu Miniflex-600 with Cu Kα radiation $\lambda\alpha = 1.5418$ Å) and the mean crystallite size (D) was estimated from the Debye–Scherrer equation: $D = \dfrac{0.90 \cdot \lambda}{\beta \cdot \cos\theta}$, where λ is the wavelength ($\lambda\alpha = 1.5418$ Å), β is the FWHM of the most intense peak (101) in the XRD pattern of samples and θ is the diffraction angle [24]. The morphological depiction of ZnO samples was obtained with FE-SEM (JEOL JSM-6360A). The elemental purity of ZnO samples was studied with EDX spectra. The optical band gap of ZnO samples was gained from UV-Visible spectra and Tauc plots obtained by UV-Visible Spectrophotometer (PerkinElmer Lambda 365). The optical properties was furthermore

deliberate with room temperature PL spectra gotten with spectrofluorometer (Shimadzu, RF-5301PC) over 300 – 700 nm range with excitation source giving 320 nm wavelength. All the PCD reactions were carried out at room temperature in solar light (natural sunlight) in batch reactor during the period of November to May. Absorbance measurement with digital colorimeter (EQUIP-TRONICS EQ-353) is used to decide the percent degradation. The maiden pH of suspension was set with the help of pH meter (LABTRONICS LT-11). Lux meter (HTC LX-100) is used for determining the light intensity.

2.4. Photocatalytic degradation experiments

The PCD efficiency of the synthesized ZnO samples was explained by means of xylenol orange dye degradation. Entire dye solutions were prepared in distilled water with diverse primary concentrations. All experiments are executed in a batch photoreactor with glass cool trap and magnetic stirrer. Xylenol Orange (100 ml) dye solution having known original concentration at appropriate pH and at room temperature was taken with known photocatalyst quantity in a cylindrical photoreactor having 7 cm height and 5 cm diameter. The even suspension of the reaction mixture was produced with ultrasonic agitation for 5 minutes. Thereafter container was kept on magnetic stirrer under solar light irradiation. At specified time intervals supernatant solution was collected and centrifuged to settle down photocatalyst particles. Then absorbance of centrifuged supernant solution was recorded at predetermined $\lambda_{\max}$ value of Xylenol Orange dye solution which is used to find the percent Degradation: $\mathrm{Deg} = \dfrac{100 \cdot [A_0 - A_t]}{[A_0]}$, where Deg is the Percent Degradation, A_0 – Initial absorbance, A_t – Absorbance at time t.

3. Result and discussion

3.1. Characterization of ZnO samples

3.1.1. Thermal gravimetric analysis. Fig. 2 shows the TG-DTA plots for zinc oxalate dihydrate (a) produced in the mechanochemical synthesis of ZnO and zinc hydroxide / hydrated zinc oxide (b) synthesized during hydrothermal assisted synthesis of ZnO. From TG-DTA curves corresponding $ZnC_2O_4 \cdot 2H_2O$, two sharp endotherms (corresponding to weight losses 18.56 and 38.52 %) are presented in the temperature range from 30 to 400 °C. The first endotherm represents loss of $2H_2O$ and second endotherm represents loss of oxalate moiety. From TG-DTA curves corresponding to $Zn(OH)_2$, two endotherms (corresponding to weight losses 13.38 and 9.18 %) are presented in the temperature range from 110 to 215 °C during the conversion of $Zn(OH)_2$ to ZnO which collectively associated with loss of water from $Zn(OH)_2$. In addition to this apparent weight loss in the temperature range 340 – 410 °C in TGA, thermogram is partly contributed to the crystallization of amorphous ZnO. From these TG-DTA curves, the suitable calcination temperature for the formation of ZnO is 450 °C for 4 hours in air atmosphere in both cases.

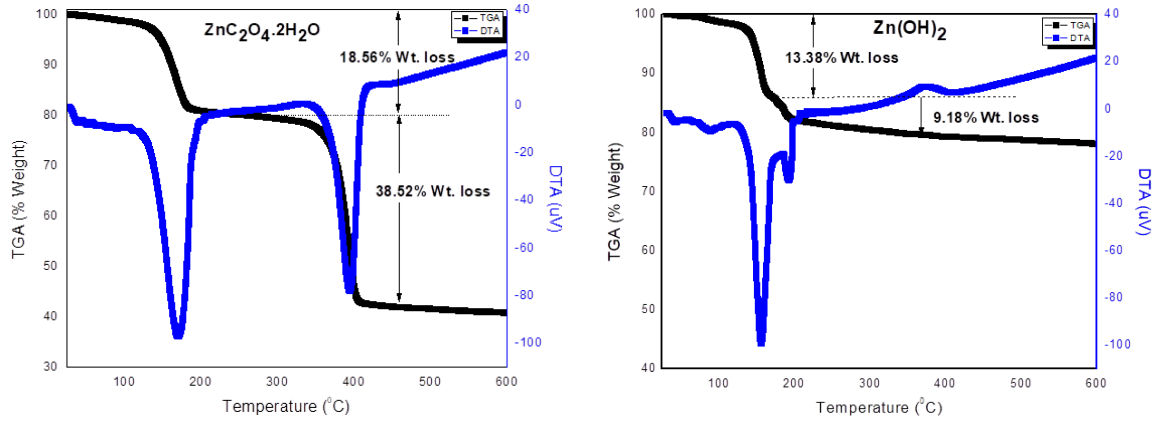

(a) (b)

FIG. 2. TG-DTA curves of $ZnC_2O_4 \cdot 2H_2O$ (a) and $Zn(OH)_2$ (b)

3.1.2. FT-IR spectroscopic study. Fig. 3 is for FT-IR spectra recorded over region 4000 – 400 cm^{-1} corresponding to the mechanochemical method (a) and hydrothermal assisted method (b) of synthesis of ZnO. In case of mechanochemical and hydrothermal routes of ZnO synthesis respectively when $ZnC_2O_4 \cdot 2H_2O$ and $Zn(OH)_2$ precursors were subjected to the calcination at 450 °C, all other bands (except those near to 450 cm^{-1}) were disappeared which were related to various symmetric and asymmetric stretching and bending vibrations in the corresponding oxalate and hydroxide precursors. This is in confirmation with the formation of pure ZnO samples [22, 25] and the same also proposed by XRD and EDS study.

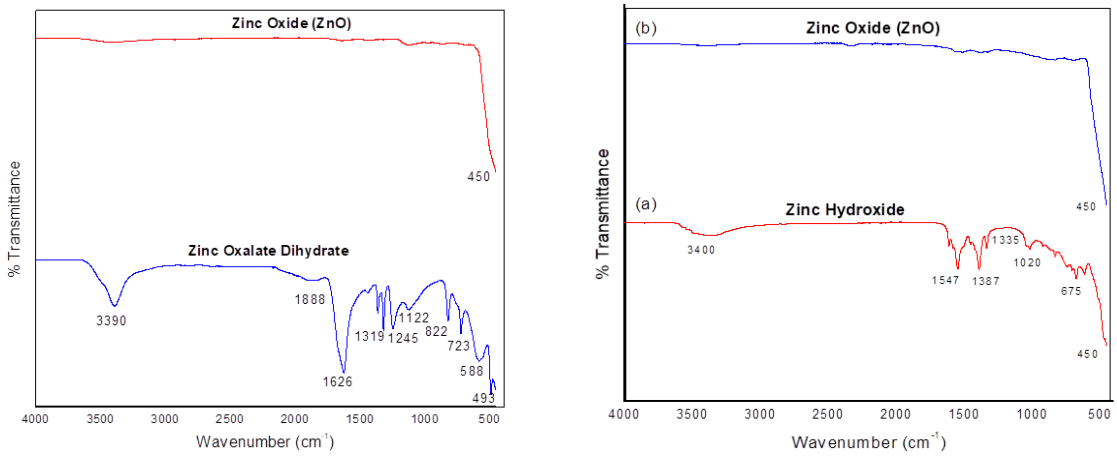

(a) (b)

FIG. 3. FT-IR spectra of mechanochemical method (a) hydrothermal method (b)

3.1.3. X-Ray diffraction (XRD) study. The XRD data for mechanochemically and hydrothermally assisted synthesized ZnO samples was collected over a 2θ range of 20° – 80° with Cu Kα radiation ($\lambda = 1.5418$ Å) display series of diffraction peaks corresponds to (100), (002), (101), (102), (110), (103), (200), (112), (201), (004) and (202) crystal planes respectively (Fig. 4) and it is in accordance with JCPDS card 36-1451 for the standard wurtzite structure of ZnO [26]. The mean crystallite size gained for mechanochemically and hydrothermally synthesized ZnO samples are 19 ± 1.0 nm and 32 ± 1.0 nm. The lattice strains deliberated by using tangent formula [27] were found to be 0.33 ± 0.005 and 0.20 ± 0.008, respectively and the specific surface areas determined by using Sauter Formula [28] were found to be 59 ± 0.40 m^2/g and 35 ± 0.20 m^2/g for mechanochemically and hydrothermally synthesized ZnO samples.

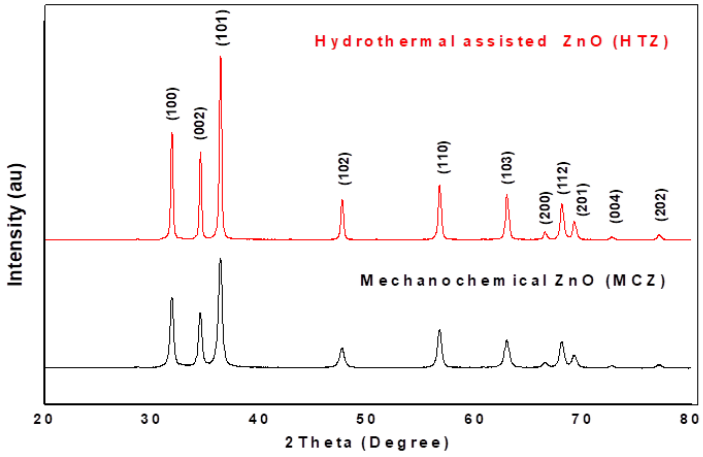

FIG. 4. XRD pattern of ZnO gained by mechanochemical (lower) and hydrothermal assisted (upper) method

3.1.4. FE-SEM study. Fig. 5 indicates the FESEM photographs of ZnO gained by mechanochemical (a) and hydrothermal assisted (b) method. The FESEM image of mechanochemically obtained ZnO shows formation of nearly homogeneous phase having non-agglomerated, dense particles of hexagonal morphology whereas the FE-SEM image of hydrothermal assisted obtained ZnO indicates the formation of particles having stacked hexagonal blocks like morphology. The mean particle sizes are found around 38 and 33 nm, respectively, for mechanochemically and hydrothermally obtained ZnO.

3.1.5. EDX analysis. Fig. 6 shows EDX spectra of ZnO samples gained by mechanochemical (a) and hydrothermal assisted (b) methods which consist of peaks corresponding to only Zn and O elements as a reflection of elemental purity of the ZnO sample. The supplementary peaks equivalent to Au, Al and C is due to their use for the preparation of conducting media to record the EDX spectra.

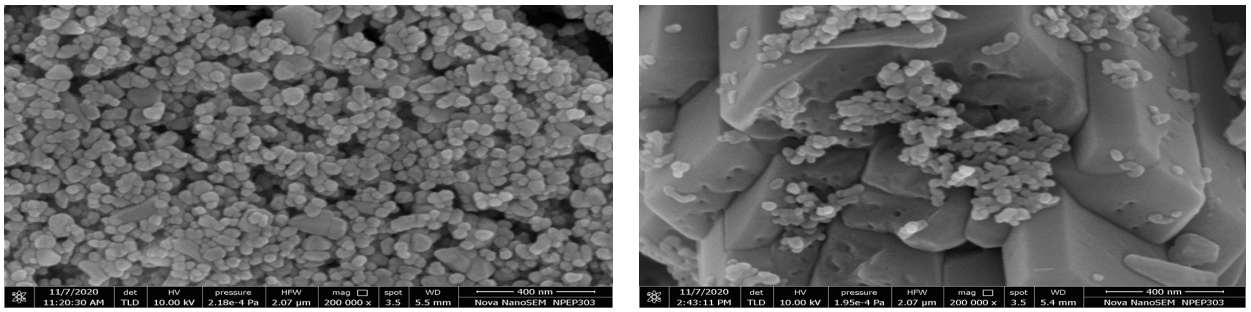

(a) (b)

FIG. 5. FESEM photographs of ZnO gained by mechanochemical (a) and hydrothermal assisted (b) method

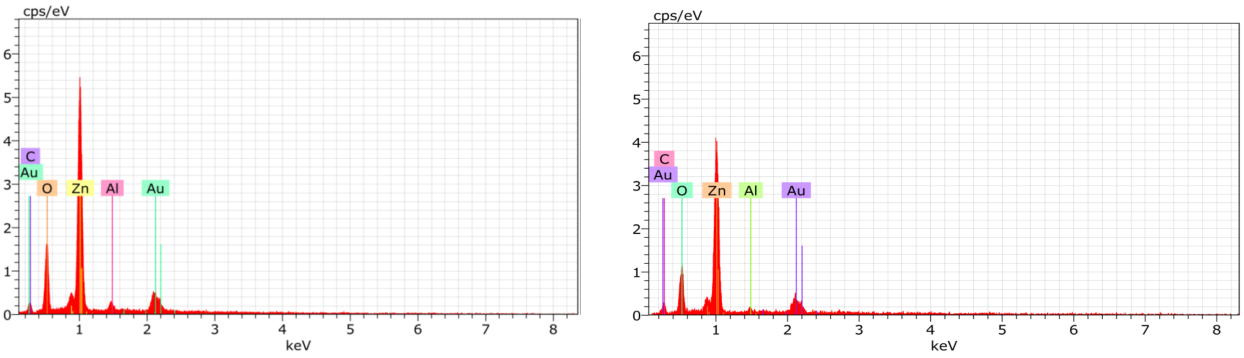

(a) (b)

FIG. 6. EDX spectrum of ZnO gained by mechanochemical (a) and hydrothermal assisted (b) method

3.1.6. UV-Visible spectra. Fig. 7(a) indicates UV-visible spectrum and Fig. 7(b) indicates Tauc plot of ZnO samples. UV-Visible spectra clearly positioned optical extinction bands in the range of 375 to 420 nm. The energy band gaps obtained using UV-visible Spectra and Tauc plots for ZnO synthesized by mechanochemical and hydrothermal assisted routes were found to be 3.16 and 3.07 eV, respectively.

3.1.7. Photoluminescence (PL) spectra. Fig. 8 shows room temperature PL spectrum of ZnO synthesized by mechanochemical method (upper red) and hydrothermal assisted method (lower green) recorded with excitation wavelength 320 nm to investigate defect in ZnO and their optical properties as well. Both ZnO samples indicate relatively weak UV (Near Band Edge) emission peaks centered near 383 nm due to free excitonic recombination matching to the band edge emission of ZnO sample [29]. Both ZnO samples also have intense green emission bands fixed near 490 nm in PL spectrum due to radiative recombination of photogenerated holes with electrons occupying oxygen vacancies [29]. Because of faster

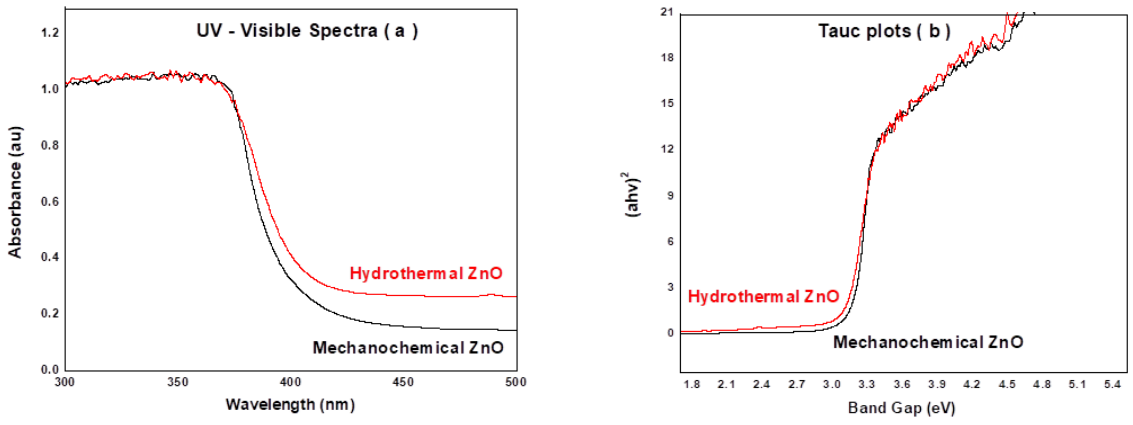

(a) (b)

FIG. 7. UV-visible spectrum (a) and Tauc plot (b) of ZnO

recombination of photogenerated hole – electron pairs, the intensity of green emission band in case of mechanochemically synthesized ZnO is more than that of hydrothermally synthesized ZnO. Also more intensity of green emission band in case of mechanochemically synthesized ZnO is in accordance with larger number of oxygen vacancies and / or defects due to the small particle size of ZnO [30].

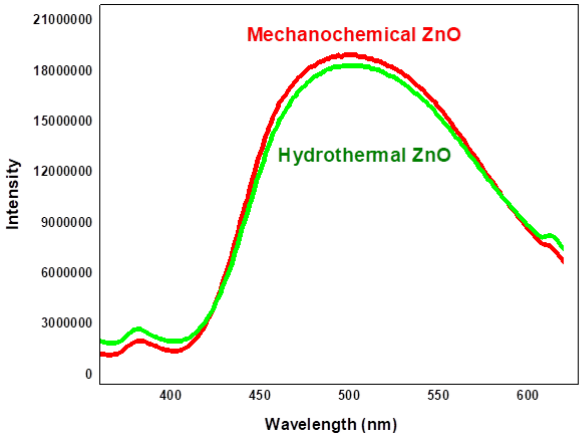

FIG. 8. Room Temperature PL spectra of ZnO samples

3.2. Photocatalytic activity of ZnO samples

Photocatalytic activity of mechanochemical and hydrothermal assistance synthesized ZnO nanomaterials and standard TiO_2 (Degussa P25) was studied with special reference to the operating parameters such as pH of dye solution, photocatalyst loading capacity, dye initial concentration, irradiation time, etc.

3.2.1. Effect of the initial pH of Xylenol Orange dye solution. The PCD of 100 ppm of Xylenol Orange dye over each of mechanochemically and hydrothermally synthesized ZnO and standard TiO_2 (Degussa P25) was deliberate at various pH from 5 to 11 with photocatalyst loading of 125 mg / 100 ml of dye solution under 6 hours of solar light irradiation (Fig. 9). The pH of the suspensions was set only prior to irradiation and set free during the course of reaction. As per fine recognized fact, slight (< 1 %) dissolution of the ZnO in acidic medium (pH 5, 6) reduces its PCD efficiency [31]. The degree of Xylenol Orange dye PCD was gradually increased with the initial pH of suspensions. Additional hydroxyl anions in alkaline medium promote photo-generation of the hydroxyl radicals (main oxidizing species) responsible for PCD [32]. Hence, PCD efficiency of ZnO samples was observed to be more at alkaline pH (9 – 11) and at pH 11 the PCD efficiency was found highest. The photocatalytic activity of hydrothermally synthesized ZnO was found quite larger than that of mechanochemically synthesized ZnO (Fig. 9).

ZnO photocatalysts obtained by both the mentioned routes show larger PCD efficiency than that of standard TiO_2 (Degussa P25) photocatalyst.

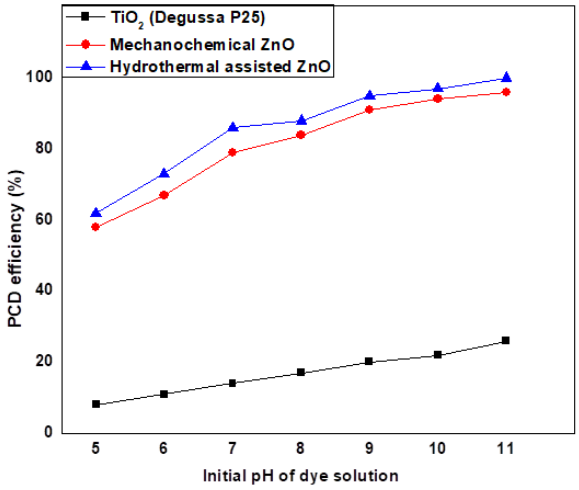

FIG. 9. Effect of the initial pH of Xylenol Orange dye solution

3.2.2. Effect of the loading of ZnO photocatalyst. The PCD of 100 ppm of Xylenol Orange over each of mechanochemically and hydrothermally synthesized ZnO samples and standard TiO_2 (Degussa P25) was deliberate at various loading amounts of photocatalyst from 50 mg / 100 ml to 175 mg / 100 ml of dye solution at pH=11 under 6 hours of solar light irradiation (Fig. 10). It was observed that, the PCD efficiency was slowly increased with ZnO loading up to particular level and acquire steadiness thereafter. The number of active sites available on the photocatalyst surface increased with its amount, hence the number of hydroxyl, and superoxide radicals also increased [22]. As a result PCD efficiency increases with ZnO loading upto 150 mg (mechanochemical) and 125 mg (hydrothermal) / 100 ml of dye solution. Beyond this limit, the PCD efficiency attains steadiness due to the availability of greater number of active species for the degradation of the same quantity of dye. Hence, 150 mg (mechanochemical) and 125 mg (hydrothermal) ZnO / 100 ml of dye solution are ample for the total degradation of Xylenol Orange within 6 hours of irradiation.

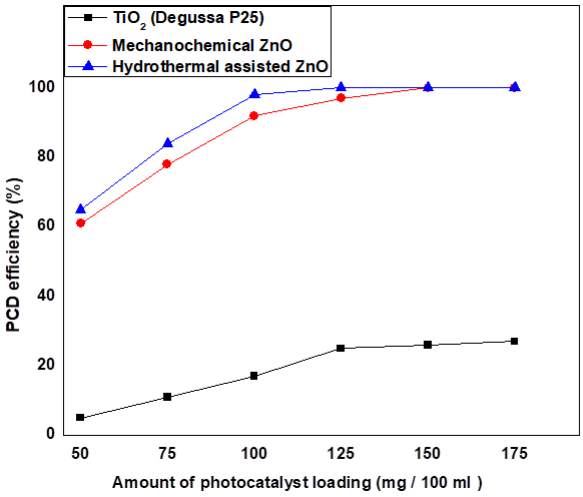

FIG. 10. Effect of the loading of ZnO photocatalyst

ZnO photocatalysts obtained by both the mentioned routes shows larger PCD efficiency than that of standard TiO_2 (Degussa P25) photocatalyst.

3.2.3. Effect of the initial concentration of Xylenol Orange dye solution. The degradation efficiency of Xylenol Orange over each of mechanochemically and hydrothermally synthesized ZnO and standard TiO_2 (Degussa P25) at different initial concentrations in the range 50 – 200 ppm was checked as a function of solar light irradiation time for 6 hours at the pH 11 of the suspension. The PCD efficiency is measured in terms of increase in percent degradation of Xylenol Orange and the results are shown in Fig. 11. The each of 50 and 75 ppm of Xylenol Orange was totally mineralized over 125 mg ZnO samples / 100 ml of the dye solution. For higher concentration of dye beyond 100 ppm the rate of PCD is higher in the case of hydrothermally synthesized ZnO than that of mechanochemically synthesized ZnO. As per the guess, increase in concentration of dye solutions decreases the extent of PCD over both ZnO samples. This is due to the formation of deep colored and turbid solution which generates obstacle in the path of light photons and hence reduces their absorption by the photocatalyst surface which results in the reduction of active radical species production responsible for the PCD. ZnO photocatalysts obtained by both the mentioned routes show higher PCD efficiency than that of standard TiO_2 (Degussa P25) photocatalyst

3.2.4. Effect of irradiation time. The PCD efficiency of mechanochemically and hydrothermally synthesized ZnO and standard TiO_2 (Degussa P25) under solar light gradually increases with increase in irradiation time (Fig. 12). 100 ml of 100 ppm Xylenol Orange dye solution was completely mineralized over 125 mg hydrothermally synthesized ZnO at the pH 11 upon 6 hours of sunlight irradiation and the rate of PCD in this case was found to be larger as compaired to that of mechanochemically synthesized ZnO.

Irradiation time directly affects the PCD efficiency. Also the ZnO photocatalysts synthesized by mechanochemical and hydrothermal assisted synthesis show higher PCD efficiency as compaired to that of standard TiO_2 (Degussa P25) photocatalyst under identical experimental conditions.

4. Conclusions

In the current research, we have described the mechanochemically and hydrothermal assisted synthesis of ZnO photocatalysts. The formation of ZnO samples from the precursor materials was confirmed by FT-IR Spectroscopy, TG-DTA, EDX and XRD technique. XRD pattern of ZnO samples matches with hexagonal wurtzite structure. Calculations based on XRD data of these samples support for larger crystallite size and smaller specific surface area and lattice strain for

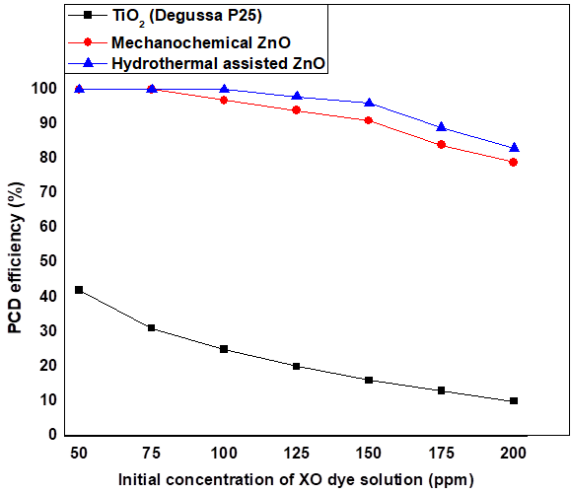

FIG. 11. Effect of the initial concentration of Xylenol Orange dye solution

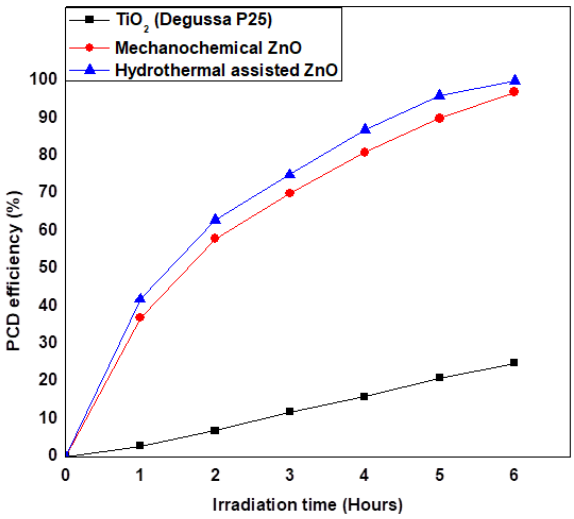

FIG. 12. Effect of irradiation time

hydrothermally synthesized ZnO sample. FE-SEM photographs indicate the formation of particles having hexagonal granular and stacked hexagonal blocks-like morphologies in case of mechanochemically and hydrothermal synthesis of ZnO samples, respectively. EDX spectra of aforementioned ZnO samples explain their elemental purity. UV-Visible and PL spectroscopies successfully explain the optical properties of ZnO nanoparticles. UV-Visible spectra gave lower bandgap energy for hydrothermally synthesize ZnO than that of mechanochemically obtained ZnO. Lower bandgap and slower recombination of photogenerated electrons and holes in case of hydrothermal ZnO may be responsible for its greater photocatalytic activity than mechanochemical ZnO. Room temperature PL spectrum of mechanochemical ZnO supports presence of more oxygen vacancies and defects which is in accordance with smaller crystallite size of the sample; but smaller photocatalytic activity of this sample may be observed due to faster recombination of photogenerated electrons and holes and large bandgap energy of this ZnO sample. The 100 ml each of 50, 75 and 100 ppm of Xylenol Orange dye solutions at pH 11 were completely mineralized over 125 mg hydrothermally obtained ZnO within 4, 5 and 6 hours of solar light irradiation, respectively. The effect of various operating factors on PCD of Xylenol Orange dye was successfully inspected.

References

[1] Aneesh P.M., Vanoja A.M., Jayaraj M.K. Synthesis of ZnO nanoparticles by hydrothermal method. In *Nanophotonic materials IV*, SPIE, 2007, **6639**, P. 47–55.

[2] Hosseini-Sarvari M. Catalytic Organic Reactions on ZnO. *Current Organic Synthesis*, 2013, **10** (5), P. 697–723.

[3] Zhu Ling, Wen Zeng. Room-temperature gas sensing of ZnO-based gas sensor: A review. *Sensors and Actuators A: Physical*, 2017, **267**, P. 242–261.

[4] Feng Hao-peng, Lin Tang, Guang-ming Zeng, Yaoyu Zhou, Yao-cheng Deng, Xiaoya Ren, Biao Song, Chao Liang, Meng-yun Wei, Jiang-fang Yu. Core-shell nanomaterials: Applications in energy storage and conversion. *Advances in Colloid and Interface Science*, 2019, **267**, P. 26–46.

[5] Madhu Rajesh, Vediyappan Veeramani, Shen-Ming Chen, Pitchaimani Veerakumar, Shang-Bin Liu, Nobuyoshi Miyamoto. Functional porous carbon–ZnO nanocomposites for high-performance biosensors and energy storage applications. *Physical Chemistry Chemical Physics*, 2016, **18** (24), P. 16466–16475.
[6] Djurišić A.B., Ng A.M.C., Chen X.Y. ZnO nanostructures for optoelectronics: Material properties and device applications. *Progress in quantum electronics*, 2010, **34** (4), P. 191–259.
[7] Liu Zi-Jheng, Jon-Yiew Gan, Tri-Rung Yew. ZnO-based one diode-one resistor device structure for crossbar memory applications. *Applied Physics Letters*, 2012, **100** (15), 153503.
[8] Rajeshkumar S., Lakshmi T., Poonam Naik. Recent advances and biomedical applications of zinc oxide nanoparticles. *Green Synthesis, Characterization and Applications of Nanoparticles*, 2019, P. 445–457.
[9] Xu Zhangliang, Yong J. Yuan. Implementation of guiding layers of surface acoustic wave devices: A review. *Biosensors and Bioelectronics*, 2018, **99**, P. 500–512.
[10] Baruah Sunandan, Joydeep Dutta. Hydrothermal growth of ZnO nanostructures. *Science and technology of advanced materials*, 2009, **10** (1), 013001.
[11] Samadi Morasae, Mohammad Zirak, Amene Naseri, Elham Khorashadizade, Alireza Z. Moshfegh. Recent progress on doped ZnO nanostructures for visible-light photocatalysis. *Thin Solid Films*, 2016, **605**, P. 2–19.
[12] Shen Liming, Ningzhong Bao, Kazumichi Yanagisawa, Kazunari Domen, Arunava Gupta, Craig A. Grimes. Direct synthesis of ZnO nanoparticles by a solution-free mechanochemical reaction. *Nanotechnology*, 2006, **17** (20), 5117.
[13] Khoshhesab Zahra Monsef, Mohammad Sarfaraz, Mohsen Asadi Asadabad. Preparation of ZnO nanostructures by chemical precipitation method. *Synthesis and Reactivity in Inorganic, Metal-Organic, and Nano-Metal Chemistry*, 2011, **41** (7), P. 814–819.
[14] Khaliullin Sh M., Zhuravlev V.D., Ermakova L.V., Buldakova L.Yu., Yanchenko M.Yu., Porotnikova N.M. Solution combustion synthesis of ZnO using binary fuel (glycine+ citric acid). *Int. J. of Self-Propagating High-Temperature Synthesis*, 2019, **28** (4), P. 226–232.
[15] Hasnidawani J.N., Azlina H.N., Norita H., Bonnia N.N., Ratim S., Ali E.S. Synthesis of ZnO nanostructures using sol-gel method. *Procedia Chemistry*, 2016, **19**, P. 211–216.
[16] Pantelitsa G., Kolokotronis K., Simitzis J. Synthesis of ZnO nanostructures by hydrothermal method. *J. of Nano Research*, 2009, **6**, P. 157–168.
[17] Azam Ameer, Faheem Ahmed, Nishat Arshi, Chaman M., Naqvi A.H. Low temperature synthesis of ZnO nanoparticles using mechanochemical route: A green chemistry approach. *Int. J. Theor. Appl. Sci.*, 2009, **1** (2), P. 12–14.
[18] Tom Asha P. Nanotechnology for sustainable water treatment – A review. *Materials Today: Proceedings*, 2021, https://doi.org/10.1016/j.matpr.2021.05.629.
[19] Tijani Jimoh O., Ojo O. Fatoba, Godfrey Madzivire, Leslie F. Petrik. A review of combined advanced oxidation technologies for the removal of organic pollutants from water. *Water, Air & Soil Pollution*, 2014, **225** (9), P. 1–30.
[20] Elamin Nazar, Ammar Elsanousi. Synthesis of ZnO nanostructures and their photocatalytic activity. *J. of Applied and Industrial Sciences*, 2013, **1** (1), P. 32–35.
[21] Kaldante Y.D., Shirsat R.N., Chaskar M.G. Photocatalytic degradation of Rose Bengal dye over mechanochemically synthesized zinc oxide under visible light irradiation. *Nanosystems: Phys. Chem. Math.*, 2021, **12** (6), P. 773–782.
[22] Pardeshi S.K., Patil A.B. Effect of morphology and crystallite size on solar photocatalytic activity of zinc oxide synthesized by solution free mechanochemical method. *J. of Molecular Catalysis A: Chemical*, 2009, **308** (1–2), P. 32–40.
[23] Liming Shen, Ningzhong Bao, Kazumichi Yanagisawa, Kazunari Domen, Arunava Gupta, Craig A. Grimes. Direct synthesis of ZnO nanoparticles by a solution-free mechanochemical reaction. *Nanotechnology*, 2006, **17**, P. 5117–5123.
[24] Aparna P.U., Divya N.K., Pradyumnan P.P. Structural and dielectric studies of Gd doped ZnO nanocrystals at room temperature. *J. of Materials Science and Chemical Engineering*, 2016, **4** (2), 79.
[25] Wahab Rizwan, Young-Soon Kim, Hyung-Shik Shin. Synthesis, characterization and effect of pH variation on zinc oxide nanostructures. *Materials transactions*, 2009, **50** (8), P. 2092–2097.
[26] Chauhan Jyotsna, Neelmani Shrivastav, Ashish Dugaya, Devendra Pandey. Synthesis and characterization of Ni and Cu doped ZnO. *J. Nanomed. Nanotechnol*, 2017, **1**, P. 26–34.
[27] Nafees Muhammad, Wasim Liaqut, Salamat Ali, Muhammad Ahsan Shafique. Synthesis of ZnO/Al: ZnO nanomaterial: structural and band gap variation in ZnO nanomaterial by Al doping. *Applied Nanoscience*, 2013, **3** (1), P. 49–55.
[28] Thangeeswari T., Parthipan G., Shanmugan S. Synthesize of gadolinium-doped ZnO nano particles for energy applications by enhance its optoelectronic properties. *Materials Today: Proceedings*, 2021, **34**, P. 448–452.
[29] Jayakumar O.D., Sudarsan V., Sudakar C., Naik R., Vatsa R.K., Tyagi A.K. Green emission from ZnO nanorods: Role of defects and morphology. *Scripta Materialia*, 2010, **62** (9), P. 662–665.
[30] Liqiang Jing, Qu Yichun, Wang Baiqi, Li Shudan, Jiang Baojiang, Yang Libin, Fu Wei, Fu Honggang, Sun Jiazhong. Review of photoluminescence performance of nano-sized semiconductor materials and its relationships with photocatalytic activity. *Solar Energy Materials and Solar Cells*, 2006, **90** (12), P. 1773–1787.
[31] Behnajady M.A., Modirshahla N., Hamzavi R. Kinetic study on photocatalytic degradation of CI Acid Yellow 23 by ZnO photocatalyst. *J. of hazardous materials*, 2006, **133** (1-3), P. 226–232.
[32] Muruganandham M., Swaminathan M. Solar photocatalytic degradation of a reactive azo dye in TiO_2-suspension. *Solar Energy Materials and Solar Cells*, 2004, **81** (4), P. 439–457.

Submitted 30 July 2022; revised 14 November 2022; accepted 27 November 2022

Information about the authors:

Yogeshwar D. Kaldante – Department of Chemistry, PDEA's Annasaheb Waghire College, Otur, Pune, Maharashtra – 412409, India; ydkaldante@gmail.com

Manohar G. Chaskar – Department of Chemistry, PDEA's Prof. Ramkrishna More College, Akurdi, Maharashtra – 411044, India; chaskarmanohar@gmail.com

Conflict of interest: the authors declare no conflict of interest.